

## Fission fragment mass reconstruction from Si surface barrier detector measurement

J.Velkovska<sup>a</sup> \* and R.L. McGrath

<sup>a</sup>Department of Physics and Astronomy, State University of New York at Stony Brook, Stony Brook, NY-11794, USA

Pacs:29.40-n,29.40Wk

A method for plasma delay and pulse-height defect corrections for Si surface barrier detectors (SBD) is presented. Based on known empirical formulae, simple approximations involving the *measured* time-of-flight (TOF) and energy of the ions were found and a mass reconstruction procedure was developed. The procedure was applied for obtaining the fission fragment mass and angular distributions from the  $^{64}\text{Ni}+^{197}\text{Au}$  reaction at 418 MeV and 383 MeV incident energy using an array of eight SBDs.

---

\*corresponding author e-mail: julia@skipper.physics.sunysb.edu , phone: (516) 632 3273 . This work was funded in part by the United States National Science Foundation.

Time-of-flight and energy measurements are the standard tool for the mass reconstruction of heavy-ion reaction products. Si detectors can provide both of these quantities for ions that are completely stopped in the detector material. A relatively simple set-up (Fig. 1) utilizing eight SBDs located at distances 50 cm and 40 cm from the target on a movable platform was used for the fragment mass and angular distribution measurement from the  $^{64}\text{Ni}+^{197}\text{Au}$  reaction at 418 MeV and 383 MeV incident energy [1]. The experiment was performed at the Stony Brook Nuclear Structure Laboratory, using  $^{64}\text{Ni}$  beam from the FN Tandem Van de Graaff and Superconducting LINAC accelerators.

However, when SBDs are used for the detection of heavy energetic fission fragments, the absolute flight-time and incident energy of the ions can not be directly determined from the measurement due to the plasma delay time  $\tau_d$  and the pulse-height defect  $E_{phd}$ . The heavy ions impinging on the detector create a dense cloud of electron-hole pairs, which can not be penetrated by the electric field generated by the bias voltage, until the cloud is dispersed by the charge diffusion. As a result, the charge collection is delayed by  $\tau_d$  with respect to the electron-hole creation time (which can be considered instantaneous). Within the dense electron-hole cloud, charge carriers can recombine with consequent loss of pulse amplitude  $E_{phd}$ , hence the total charge collected from the detector is no longer proportional to the ion's energy. For the reactions studied above,  $\tau_d$  was between 0.2 - 1.5 ns and  $E_{phd}$  - up to 25 MeV. Large corrections to the measured TOF and energy  $E_{det}$  were needed for the successful mass reconstruction.

Although systematic studies of the above effects exist in the literature [2,3], the empirical formulae that are derived relate  $\tau_d$  and  $E_{phd}$  to the *unknown* mass A, charge Z and incident energy  $E = E_{det} + E_{phd}$  of the ions:

$$\tau_d = \frac{\bar{Z}^2}{2A} \exp\left(\frac{-E}{3.75A}\right) C \left(\frac{\rho}{d}\right)^{\frac{2}{5}} \frac{1}{F_{eff}}, \quad (1)$$

$$E_{phd} = 2.33 \times 10^{-4} (AZ)^{\frac{6}{5}} (E/A)^{\frac{1}{2}} \times \left[ 1 + \frac{1.32 \times 10^3 Z (S/E^2)^{\frac{1}{3}}}{\rho^{\frac{1}{4}} F_{eff}} \right] \quad (2)$$

Here,  $\bar{Z} \approx \sqrt{(dE/dx)_{ion} / (dE/dx)_{proton}}$  (charge units) is the effective charge of the ion, expressed in terms of the stopping power of the ion and a proton at the same velocity,  $d$  (cm) - the detector thickness,  $\rho$  ( $\Omega \cdot \text{cm}$ ) - the detector resistivity,  $C$  (pF) - the capacitance of the totally depleted detector,  $S$  - the stopping power in the detector material in MeV/(mg/cm<sup>2</sup>). The effective field strength  $F_{eff}$  (V·cm) is given by:

$$F_{eff}(x) = (d - x)/\mu\tau, \quad (3)$$

where  $d \approx \sqrt{2\tau\mu V}$  is the depletion depth at a given bias voltage  $V$ ,  $\mu \approx 1481 \text{ cm}^2\text{V}^{-1}\text{s}^{-1}$  is the constant electron mobility,  $\tau \approx \rho \times 10^{-12}\text{s}$  and  $x$  is taken at the charge centroid of the ionized track produced by the heavy ion (about 1/3 of the ion range in the material). Some relevant quantities for the detectors used in this experiment are given in Table 1.

Being able to calculate  $\tau_d$  and  $E_{phd}$  from the above equations does not guarantee that the necessary corrections to the measured TOF and  $E_{det}$  can be made, since finding analytic solutions to the inverse problems is extremely complicated. In this work, approximate solutions which are simple, accurate to 5% and derived directly from the measured quantities are described.

The plasma delay time was calculated from equation (1) for ions with masses and energies within the range of the experiment. Figure 2(a) shows the delay time for the projectile  $^{64}\text{Ni}$ , the recoil  $^{197}\text{Au}$  and for the symmetric fragments  $A=130$  as a function of incident energy. There is no unique functional dependence on the incident energy for the different ions of interest, hence the energy information from the measurement can not be used to correct the measured TOF. However, if we plot the “true” velocity of the ions as a function of the measured velocity  $V_{det} = \text{flight\_distance}/(\text{TOF} + \tau_d)$  (Fig.2(b)), for all ions in the range of the experiment, there is one linear function giving the relation between the “true” and the measured velocity. The fitted line and the fit parameters are shown in Fig.2(b). Thus using equation (1) and the geometry of the particular experiment, one can extract a linear correction to the measured velocity.

After applying the velocity corrections, we need to account for the pulse-height defect in order to reconstruct the ion mass using equation (2) and the measured energy  $E_{det} = E - E_{phd}$ . Although deriving an equation for the mass  $A$  involving the corrected velocity and other known quantities is in principle possible, its analytic solution is a formidable task. The following simple procedure was developed instead:

The pulse-height defect was calculated (from equation (2)) for the masses and energies covered in the range of the experiment. Assuming that the charge-to-mass ratio in the fragments is equal to the charge-to-mass ratio in the composite system, the dependence on the velocity for constant mass was extracted. Figure 3 shows the constant mass curves: they show linear dependence of  $E_{phd}$  on the velocity. Only for  $V_{true} < 0.02c$  a deviation from linearity is observed. This imposed a velocity cut in the data analysis. Linear fits were applied to the calculated constant mass curves:  $E_{phd}(V_{true}) = a(A) + b(A) \cdot V_{true}$ . The coefficients  $a(A)$  and  $b(A)$  at fixed mass were extracted for  $A=70-180$  in steps of 10 mass units.

After factoring out the velocity dependence, the mass dependence of the coefficients  $a(A)$  and  $b(A)$  was examined. They were found to depend quadratically on mass. The quadratic fits are shown in panel (b) and (c) of Figure 3. With the parameters extracted from the above fits, we can write a quadratic equation for the mass of the ion, involving only *measured* quantities:

$$E_{det} + \left[ a_1 + a_2 A + a_3 A^2 + (b_1 + b_2 A + b_3 A^2) V_{true} \right] = \frac{A V_{true}^2 u}{2} \quad (4)$$

Here  $V_{true}$  is the “true” velocity, which was previously determined as a function of the measured velocity  $V_{det}$  and  $u = 931.5$  MeV is the nucleon mass.

A computer simulation was developed to test this procedure. Fission fragments from the  $^{64}\text{Ni} + ^{197}\text{Au}$  reaction at 418 MeV were generated with a known mass  $A$  and Viola systematics kinetic energy. The laboratory energy and TOF were calculated for each detector position. Using equations (1) and (2) the plasma delay and the pulse-height defect were calculated. Then  $E_{det}$  and  $V_{det}$  were obtained, and following the outlined procedure, the “unknown” mass of the fragments was recovered. The solution of equation (4) gave very accurate results for light masses (within 1.5 mass units) and somewhat poorer results for the heaviest masses (within 5 units of the input).

Another technical detail, that is crucial for this measurement is the absolute energy and time calibration of the detectors and the subsequent electronics. The energy cali-

bration was done using several reference signals: The low energy part of the spectrum was calibrated using a  $^{228}\text{Th}$   $\alpha$ - source. Detectors 1-5 in the forward position (covering from  $20^\circ$  to  $90^\circ$  in the laboratory system) were within the grazing angle for the  $^{64}\text{Ni} + ^{197}\text{Au}$ ,  $E_{lab} = 418$  MeV reaction, so the elastic peak could be used as a calibration point. A low energy calibration run at 247 MeV provided additional calibration points. At this energy, with the platform in forward position, all SBDs could detect Rutherford scattering. Fig. 4 shows the TOF and the energy spectra in all eight detectors at this energy. It is interesting to note, that in SBD 1-5 the recoil  $^{197}\text{Au}$  is also seen. These points, wherever present, were included in the calibration as well. The energy resolution was  $\sim 2\%$  for the elastically scattered beam and  $\sim 1.2\%$  for  $\alpha$ -particles.

To calibrate the timing one needs to relate the channel number of the TOF spectrum to the actual TOF through a linear function. The slope was determined reliably using the reference RF signal of the LINAC accelerator. Determining the absolute offset is more difficult, because at the high energy only the first 5 detectors could see elastically scattered beam, for which the TOF is known absolutely. The 247 MeV run gave the relative timing between the detectors, so SBDs 6,7,8 could also be calibrated. The Full-Width-at-Half-Maximum of the beam pulse coming from the accelerator was  $\leq 600ps$ . Corrections were made for the plasma delay time of the heavy fragments, and the overall timing resolution for the elastic reaction products measured was  $\leq 1ns$ .

After completing the time and energy calibrations, we have all the ingredients needed for the mass reconstruction procedure. One should note, that it has built-in the assumption that the reaction products are coming from the target (which is at a known distance from the detector), so care should be taken that noise events do not enter the reconstruction. Figure 5(a) shows an example of a scatter plot of uncalibrated energy versus TOF from detector 3, located at  $40^\circ$  in the lab, from the 418 MeV measurement. The reaction products of interest are separated from the slit scattered beam and low pulse-height noise using a “banana” gate. Only the gated events are reconstructed. Figure 5(b) shows the reconstructed mass spectrum. Combining all experimental uncertainties, the mass reconstruction was estimated to be accurate to  $\leq 10$  mass units.

## REFERENCES

1. J. Velkovska, C. R. Morton, R. L. McGrath, P. Chung, and I. Diószegi. *Phys. Rev.*, C 59:1518, 1999.
2. W. Bohne, W. Galster, K. Grabishc, and H. Morgenstern. *Nucl. Instr. and Meth.*, A240:145, 1985.
3. M. Ogihara, Y. Nagashima, W. Galster, and T. Mikumo. *Nucl. Instr. and Meth.*, A251:313, 1986.

Table 1  
BF-028-400-60 detector characteristics

Detector Model	Nominal
BF-028-400-60	Characteristics
Active area [mm <sup>2</sup> ]	400
Resistivity [ $\Omega \cdot cm$ ]	490
Thickness [cm]	0.006
Capacitance [pF]	163
Nominal bias voltage [V]	64
Effective field strength at nominal bias [V/cm]	12362
Bias voltage applied [V]	100
Effective field strength at 100 V bias [V/cm]	15680

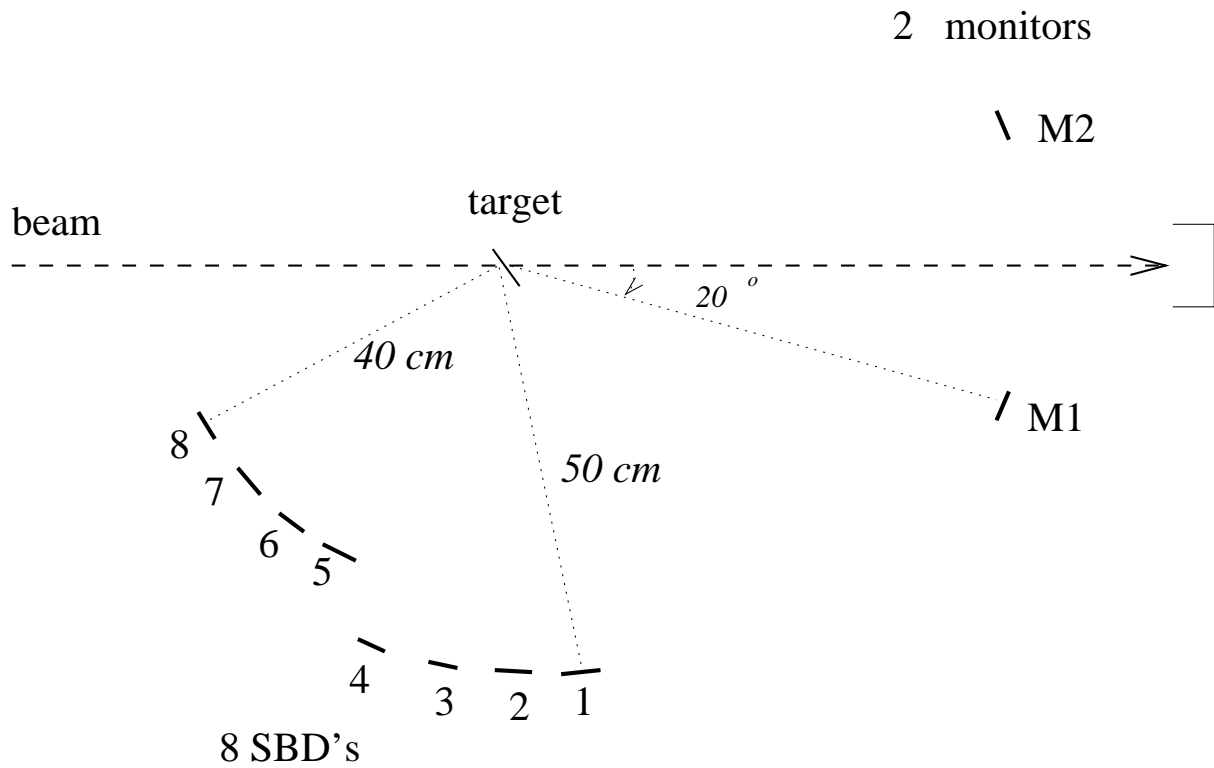


Figure 1. Experimental set-up used for fragment mass and angular distribution measurement from the  $^{64}\text{Ni}+^{197}\text{Au}$  reaction at 418 MeV and 383 MeV incident energy. Eight SBDs model EG&G ORTEC BF-028-400-60 were placed on a movable platform  $10^\circ$  apart. Measurements were taken at two positions of the platform covering from  $20^\circ$  to  $90^\circ$  and from  $80^\circ$  to  $150^\circ$  in the laboratory system.

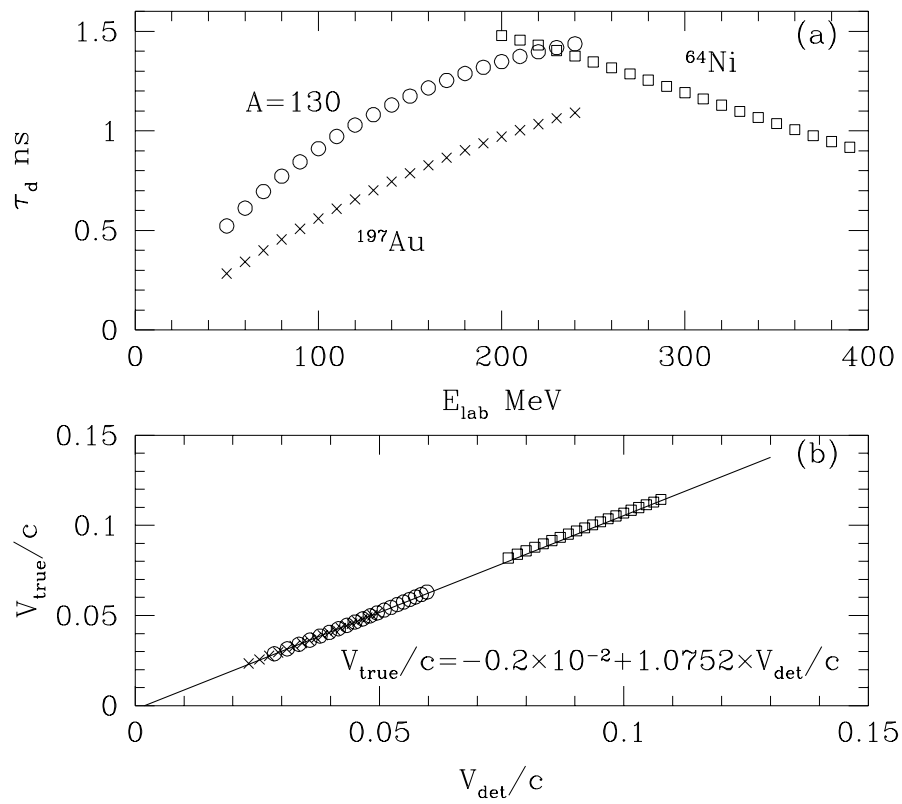


Figure 2. (a) Plasma delay time for selected ions as a function of incident energy. (b) The true velocity  $V_{true}$  as a function of the experimentally accessible velocity  $V_{det}$  with the fitted linear expression.

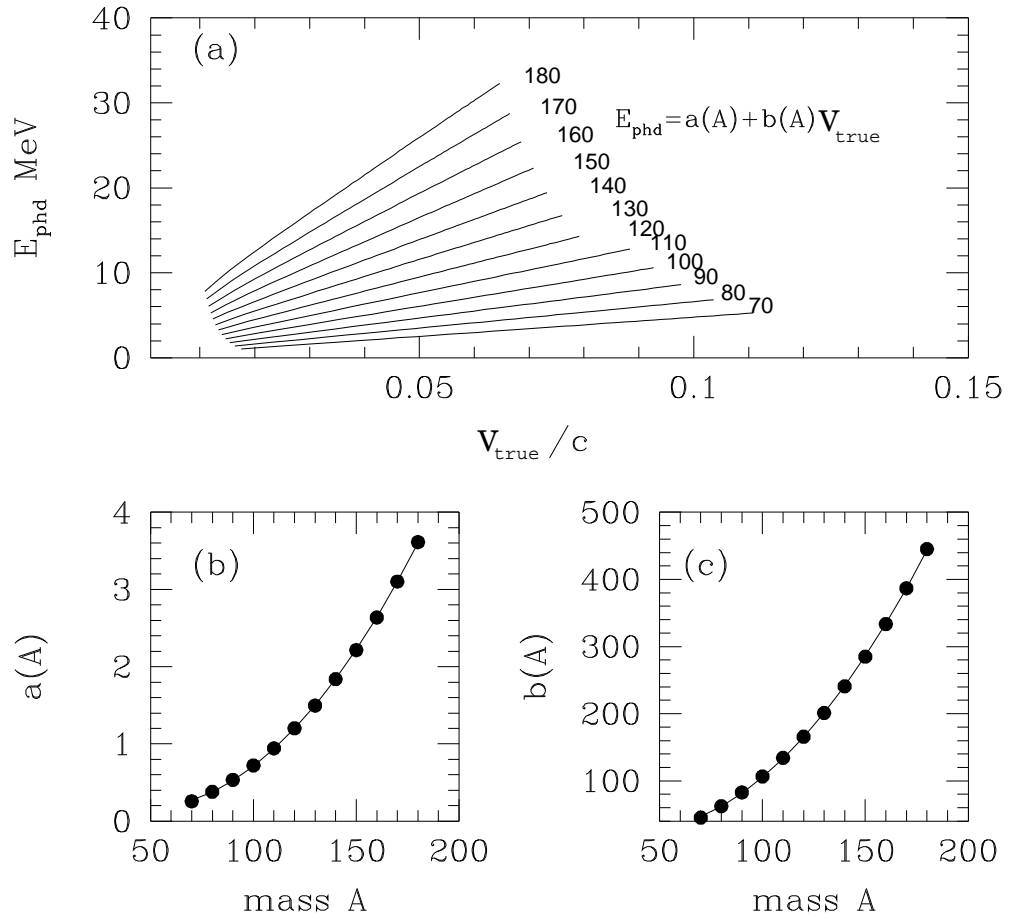


Figure 3. (a) Constant mass curves of pulse-height defect as a function of velocity. (b),(c) The coefficients of the linear fits (points)  $E_{\text{phd}}(V_{\text{true}})$  and the quadratic fits to their mass dependence (lines).

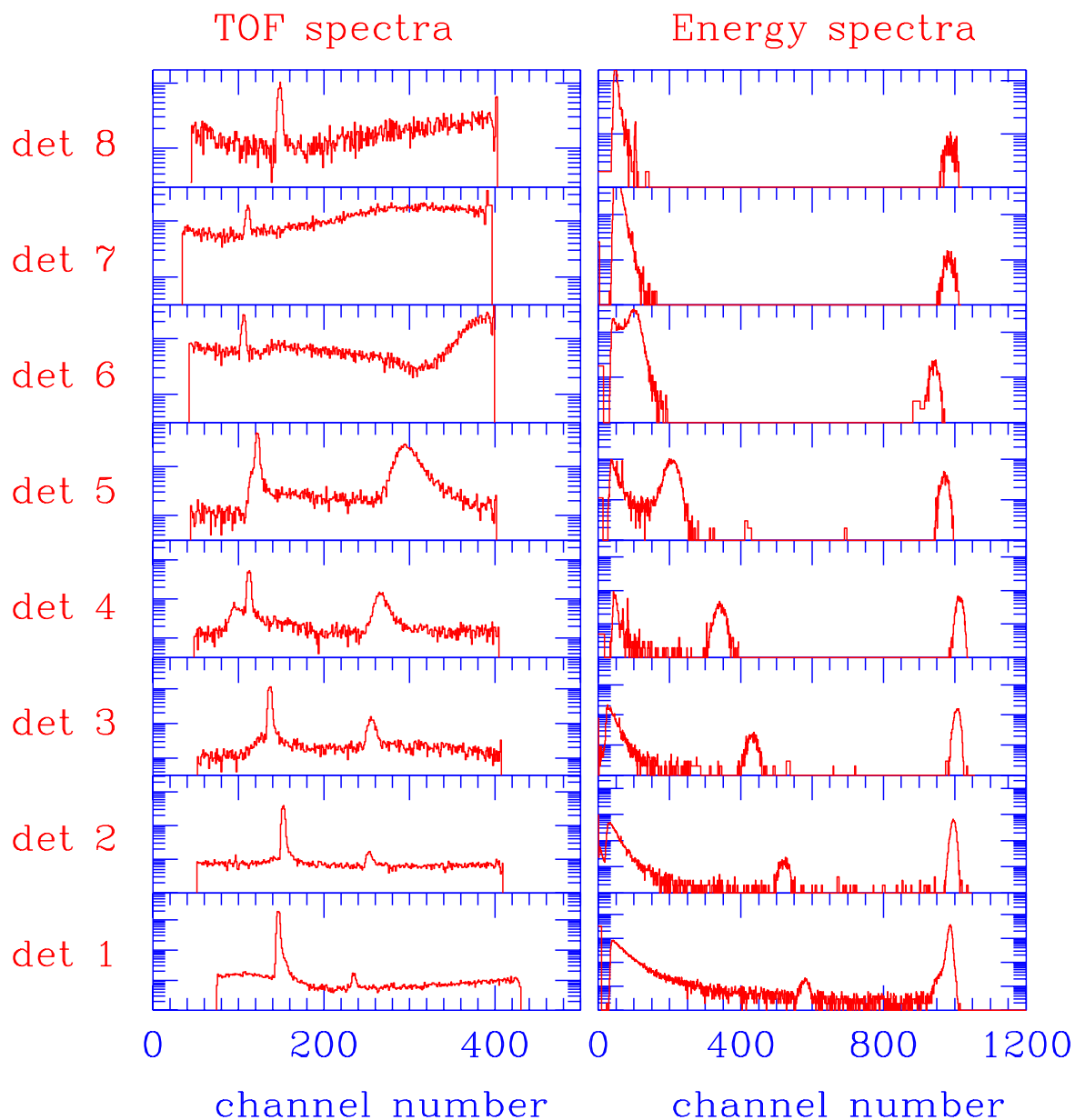


Figure 4. TOF and energy spectra in the fission-fragment detectors from the 247 MeV calibration run. The sharp peaks in the TOF spectra come from the elastically scattered  $^{64}\text{Ni}$ . The broad peaks to the right are the recoil  $^{197}\text{Au}$ . In the energy spectra, the elastic  $^{64}\text{Ni}$  is at channel  $\sim 1000$ . The lower peaks come from  $^{197}\text{Au}$ .

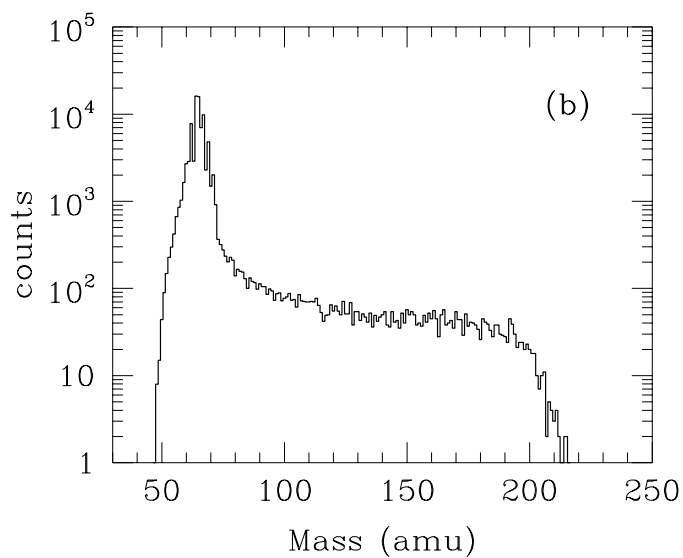
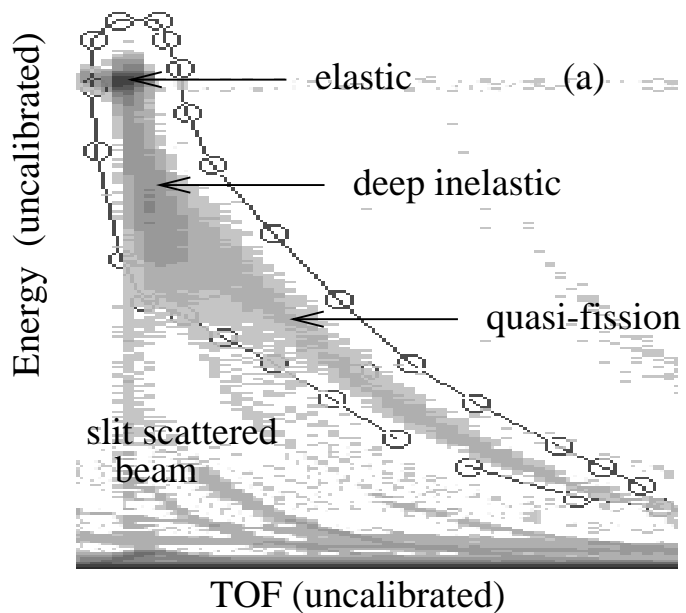


Figure 5. (a) Energy versus TOF (uncalibrated) scatter plot from detector 3 located at  $40^\circ$  in the lab system for  $E_{lab} = 418$  MeV. The “banana” gate is applied to select the reaction products of interest. (b) Mass reconstruction for the gated events. The peak in the spectrum is the elastically scattered  $^{64}\text{Ni}$ .